JOURNAL OF Materials CHEMISTRY

Magnetic properties of phosphate-bridged copper(II) organic–inorganic hybrid compounds

Yanko Moreno,[a] Andrés Vega,[a] Svetlana Ushak,[b] Ricardo Baggio,[c] Octavio Peña,[d] Eric Le Fur,[e] Jean-Yves Pivan[e] and Evgenia Spodine*[a,b]

[a]*Centro para la Investigación Interdisciplinaria Avanzada en Ciencia de los Materiales (CIMAT), Universidad de Chile, Santiago, Chile*
[b]*Facultad de Ciencias Químicas y Farmacéuticas, Universidad de Chile, Casilla 233, Santiago, Chile*
[c]*Comisión Nacional de Energía Atómica, Buenos Aires, Argentina*
[d]*Laboratoire de Chimie du Solide et Inorganique Moléculaire UMR-CNRS 6511, Institut de Chimie de Rennes, Université de Rennes 1, 35042 Rennes CEDEX, France*
[e]*Laboratoire de Physicochimie, Ecole Nationale Supérieure de Chimie de Rennes, Institut de Chimie de Rennes, 35700 Rennes, France. E-mail: espodine@ciq.uchile.cl*

Received 16th December 2002, Accepted 10th July 2003
First published as an Advance Article on the web 29th July 2003

Hydrothermal synthesis has allowed us to isolate and characterize three new inorganic–organic hybrid materials, the compounds $[Cu_2(phen)_2(H_2O)_2(H_2PO_4)_2](NO_3)_2{\cdot}2H_2O$ (**1**), $[(Cu_2bipy_2)_2(V_4O_9)(PO_4)_2(HPO_4)(H_2P_2O_7)]_n{\cdot}nH_2O$ (**2**) and $[Cu_2(dpa)_2(V_2P_2O_{12})]_n$, (**4**), which have been magneto-structurally characterized. In addition, the magnetic behaviour of the related compound $[Cu_2(bipy)_2(VO_2)_2(PO_4)_2]_n$ (**3**), has been measured. Compound **1** has a dimeric structure, while compound **2** and **4** have dimer chain structures. The dependence of the magnetic susceptibility on temperature suggests antiferromagnetic coupling for **1**, **2** and **3**, while compound **4** can be well understood in terms of the Curie–Weiss law with $\theta = -23$ K. The fitting of the magnetic behaviour to the Bleaney–Bowers spin–dimer coupling expression leads to $J = -8.0$ cm^{-1} for **1**, $J = -28.8$ cm^{-1} for **2** and $J = -29.0$ cm^{-1} for **3**. The use of alternating chain expressions leads to $J = -28.8$ cm^{-1}, $\alpha = -0.03$ for **2** and $J = -29.4$ cm^{-1}, $\alpha = -0.027$ for **3**.

Although a variety of coordination geometries are exhibited by the compounds in the series, all of them have O–P–O bridges connecting the cupric centres. It was possible to identify the role of the vanadyl groups of the phosphovanadate framework as an important factor affecting the ability of the phosphate groups to transmit magnetic interactions.

Introduction

The $VOH_xPO_4^{(3-x)-}$ system has numerous structures which range from molecular species to three dimensional structures. Among them, two dimensional lamellar compounds (2D) have been specially well studied since they undergo intercalation reactions with diverse range of species.[1–4] The diversity of oxidation states and vanadium polyhedra (octahedra, pyramids, tetrahedra) and the diversity of ways in which these can be connected to the $H_xPO_4^{(3-x)-}$ tetrahedra, provide the basis for the preparation of structurally unprecedented oxovanadium phosphate compounds. The use of hydrothermal techniques has allowed a large number of these materials to be obtained. When organic components that possess structure-directing properties are introduced into the reaction mixture a remarkable array of metastable inorganic–organic composite oxides is obtained. These new compounds retain some of the structural features of the synthetic precursors. The organic components can act as charge compensating cations,[5–9] or as ligands which are covalently linked to the inorganic backbone of the solid.[10,11] Recently there has been considerable interest in the use of coordination complexes as structure directing agents.[12–16] The main advantage of this strategy lies in the variety of shapes and charges presented by the complexes, as well as in the possibility of introducing a transition metal into the oxide structure. The coordination preferences of the transition metal centre will produce the necessary structural modifications of the V–P–O structures. Thus the use of copper(II) complexes with 2,2′-bipyridine (bipy), 2,2′-dipyridylamine (dpa) and 1,10-phenanthroline (phen) ligands are expected to change the 3D or 2D arrays to 0D and 1D structures, permitting the study of low dimensional magnetic phenomena. In contrast to the more extensively studied bipy ligand the dpa ligand is particularly attractive since the NH group between the two pyridyl rings permits the stabilisation of the structure through hydrogen bonding interactions, while the phen molecule allows the consequence of the steric constraints of the ligand to be investigated.

As an extension to this synthetic approach to organic–inorganic hybrid oxides, we herein report the synthesis and structure determination of new Cu(II) oxovanadium(V)–phosphate diimine compounds [diimine: 2,2′-bipyridine (bipy), 2,2′-dipyridylamine (dpa) and 1,10-phenanthroline (phen)]: $[Cu_2(phen)_2(H_2O)_2(H_2PO_4)_2](NO_3)_2{\cdot}2H_2O$ (**1**), $[(Cu_2bipy_2)_2(V_4O_9)(PO_4)_2(HPO_4)(H_2P_2O_7)]_n{\cdot}nH_2O$ (**2**) and $[Cu_2(dpa)_2(V_2P_2O_{12})]_n$, (**4**). The magnetic susceptibility data of these three compounds are also described, together with that of the related solid $[Cu_2(bipy)_2(VO_2)_2(PO_4)_2]_n$ (**3**), the structure of which was reported by Feng *et al.*[16]

Experimental

Reagents were purchased from Aldrich Chemical Co. and Fluka, and were used without further purification. All syntheses were

Table 1 Summary of crystal data and refinement details for $[Cu_2(phen)_2(H_2O)_2(H_2PO_4)_2](NO_3)_2{\cdot}2H_2O$ (**1**), $[(Cu_2(bipy)_2)_2(V_4O_9)(PO_4)_2(HPO_4)(H_2P_2O_7)]_n{\cdot}nH_2O$ (**2**) and $[(Cu(dpa))_2(V_2P_2O_{12})]_n$ (**4**)

	1	**2**	**4**
Formula	$Cu_2C_{24}H_{28}N_6O_{18}P_2$	$Cu_4C_{40}H_{0.35}N_8O_{29}P_5V_4$	$CuC_{10}H_9N_3O_6PV$
Mol. Wt	877.5	1722.52	412.65
Cryst. System	Triclinic	Triclinic	Triclinic
Space group	$P\bar{1}$	$P\bar{1}$	$P\bar{1}$
a/Å	7.1367(6)	7.413(1)	7.3914(17)
b/Å	10.615(1)	12.9922(5)	9.863(2)
c/Å	11.063(1)	14.9682(5)	10.311(2)
α/°	85.541(1)	87.80(1)	107.030(4)
β/°	83.150(1)	78.85(1)	105.119(4)
γ/°	70.652(1)	78.09(1)	98.158(4)
V/Å^3	784.5(1)	1383.9(7)	674.1(3)
Z	1	1	2
D_c/g cm^{-3}	1.858	2.063	2.033
F(000)	446	843	410
μ(Mo-Kα)/mm^{-1}	1.552	2.398	2.422
Reflns, unique/obs	3292/2652	5852/1808	2816/1260
R^b	0.0347	0.0682	0.0570
$R_w{}^c$	0.0426	0.0887	0.0888
S^d	0.9500	0.95	0.7650
Max. diff. e. dens./e Å^3	0.453; −0.340	1.25; −0.71	0.495; −0.453

[a]Details in common: T = 25 °C, $I > 2\sigma(I)$. [b]$R = \Sigma(||F_o| - |F_c||)/\Sigma|F_o|$. [c]$R = [\Sigma w(||F_o| - |F_c||)^2/\Sigma|F_o|^2]^{1/2}$. [d]Goodness of fit = $[\Sigma w(|F_o| - |F_c|)^2/\Sigma("_o - N_p)]^{1/2}$.

carried out in 23 mL poly(tetrafluoroethylene)-lined stainless steel containers under autogenous pressure.

a) Syntheses

$[Cu_2(phen)_2(H_2O)_2(H_2PO_4)_2](NO_3)_2{\cdot}2H_2O$ (1). A mixture of $Cu(NO_3)_2{\cdot}3H_2O$ (0.416 g, 1.72 mmol), V_2O_5 (0.153 g, 0.84 mmol), 1,10-phenanthroline (0.6727 g, 3.397 mmol), H_3PO_4 (8.7 mmol) and H_2O (230 mmol) was heated at 120 °C for 72 h, and then the temperature was slowly lowered to 80 °C (10 °C h^{-1}). After the reaction vessel was cooled to room temperature, blue crystals of **1** were collected. Anal. Calcd: C, 32.8; H, 3.2; N, 9.7%. Found: C, 33.1; H, 3.2; N, 10.0%.

$[(Cu_2bipy_2)_2(V_4O_9)(PO_4)_2(HPO_4)(H_2P_2O_7)]_n{\cdot}nH_2O$ (2). A mixture of $Cu(NO_3)_2{\cdot}3H_2O$ (0.416 g, 1.72 mmol), V_2O_5 (0.155 g, 0.85 mmol), 2,2′-bipyridine (0.530 g, 3.39 mmol), H_3PO_4 (8.7 mmol), H_2O (230 mmol) and Zn (0.112 g, 1.77 mmol) was heated at 120 °C for 72 h, and then the temperature was slowly lowered to 80 °C (10 °C h^{-1}). Blue crystals of **2** (Anal. Calcd: C, 28.1; H, 2.2; N, 6.5%. Found: C, 28.5; H, 2.3; N, 6.8%) were obtained as a minor product upon cooling, together with two other crystallised phases present as yellow–brown needle-like and blue prismatic crystals. X-Ray diffraction shows that the yellow crystals correspond to a vanadium dimer $[(VO_2)_2(bipy)_2(PO_3OH)]$, which is isoformular and has the same connectivity as the one previously reported by Zubieta *et al.*,[17] but with a different packing pattern: hydrogen bonded chains instead of the hydrogen bonded dimers of dimers described by Zubieta. Our vanadium(v) complex crystallises in the monoclinic system, $C2/c$ space group, with a = 13.9768(16) Å, b = 22.157(3) Å, c = 9.1984(10) Å and β = 103.165(2)°. †

In the same way, single crystal X-ray diffraction shows that the blue prismatic crystals correspond to $[Cu_2(bipy)_2(VO_2)_2(PO_4)_2]_n$, **3**, as previously reported by Feng *et al.*[16] In this paper we report the magnetic behaviour of this compound.

In general, since the hydrothermal syntheses are subject to kinetic control, there is no apparent correlation between the starting composition and the stoichiometry of the obtained crystalline products.

$[Cu_2(dpa)_2(V_2P_2O_{12})]_n$ (4). A mixture of $Cu(NO_3)_2{\cdot}3H_2O$ (0.406 g, 1.68 mmol), V_2O_5 (0.153 g, 0.84 mmol), 2,2′-dipyridylamine (0.575 g, 3.36 mmol), H_3PO_4 (8.7 mmol), H_2O (230 mmol) and Zn (0.106 g, 1.62 mmol) was heated at 120 °C for 72 h, and then the temperature was slowly lowered to 80 °C (10 °C h^{-1}). Green needles of **4** were collected by manual separation under a microscope from a mixture of blue and black powders. Anal. Calcd: C, 29.1; H, 2.2; N, 10.2%. Found: C, 28.7; H, 2.4; N, 10.2%.

b) Structure determination. Plates of **1** (0.2 × 0.2 × 0.05 mm) and **2** (0.07 × 0.06 × 0.02 mm), and a needle shaped crystal of **4** (0.09 × 0.06 × 0.05 mm) were mounted on a glass fiber. The intensity collection was made on a Bruker SMART APEX diffractometer, using a separation of 0.3° between frames and for 10 s per frame. Data integration was made using SAINT.[18] The structures were solved using XS in SHELXTL[19] by means of direct methods, completed by Fourier difference synthesis and refined until convergence using XL SHELXTL[19] and SHELXL97.[19] In the case of **2** the starting structure model was extracted by direct methods using SIR97[20] and the refinements were made on F_o^2 with Jana2000.[21] For additional data collection and refinement details, see Table 1.

c) Magnetic susceptibility measurements. The magnetisation of **1–4** was measured under a constant applied field (1 or 2 kOe) within a temperature range of 5–300 K with a SHE VTS-906 SQUID susceptometer–magnetometer. Complementary magnetic data for compound **2** was also recorded at low temperatures (2–10 K). All the experimental data were corrected by diamagnetic contributions and temperature independent paramagnetism of copper(II) (TIP = 60 × 10^{-6} emu per Cu atom).

Results and discussion

a) Structural description

$[Cu_2(phen)_2(H_2O)_2(H_2PO_4)_2](NO_3)_2{\cdot}2H_2O$ (1). Fig. 1a shows the structure of **1**. It is a μ_2-diphosphate copper(II) dimer that crystallises in the triclinic crystal system, space group $P\bar{1}$. Two $Cu(phen)(H_2O)^{2+}$ units are bridged by two phosphate anions in a μ_2-fashion, in such a way as to define a distorted square pyramidal geometry around each copper centre, with two nitrogen atoms from the chelating phen and two phosphate

†CCDC reference numbers 200041–200042 and 208664. See http://www.rsc.org/suppdata/jm/b2/b212463g/ for crystallographic files in CIF or other electronic format.

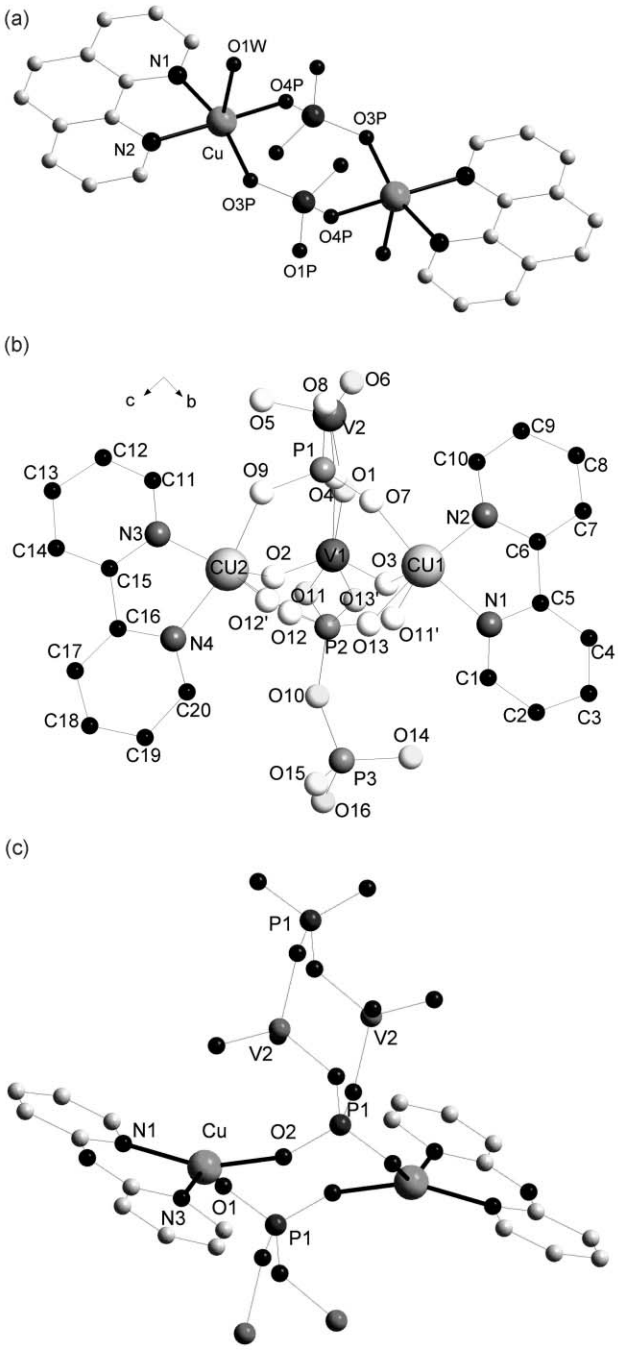

Fig. 1 Molecular structure diagrams for a) $[Cu_2(phen)_2(H_2O)_2(H_2PO_4)_2](NO_3)_2{\cdot}2H_2O$ (**1**), b) $[(Cu_2(bipy)_2)_2(V_4O_9)(PO_4)_2(HPO_4)(H_2P_2O_7)]_n{\cdot}nH_2O$ (**2**) and c) $[(Cu(dpa))_2(V_2P_2O_{12})]_n$ (**4**).

oxygen atoms in the basal positions, and a water oxygen atom occupying the apical one. An inversion centre relates the two copper centres in the dimer, which implies that the H_2PO_4 groups are located in a chair-like arrangement at different sides of the coordinated phosphate oxygen mean plane. The copper centre is displaced *ca.* 0.15 Å towards the apical oxygen at 2.308(2)Å. The basal distances are Cu–N1, 2.019(2); Cu–N2, 2.021(2); Cu–O(3P), 1.920(1) and Cu–O(4P), 1.941(1) Å. The phosphate group shows a lengthening of the P–OH bond lengths (mean 1.559(2) Å) due to protonation. The distance between the two copper(II) centres inside the dimer is 5.010(1) Å. The two copper coordination planes are parallel, but not coplanar.

The two nitrate anions provide charge counterbalance; together with a couple of hydration water molecules and the cationic dimer units, they define a profuse 2D H-bonding network parallel to the plane (001) (Fig. 2a). Interactions along the ***c*** direction are much weaker and consist of van der Waals bonds between the aromatic groups. Table 2 shows some bond distances, angles and dihedral angles for **1**.

$[(Cu_2(bipy)_2)_2(V_4O_9)(PO_4)_2(HPO_4)(H_2P_2O_7)]_n{\cdot}nH_2O$ (2). The fundamental structural motif of this compound is shown in Fig. 1b. The coordination sphere around each copper(II) is defined by two bipy nitrogen atoms, two phosphorus oxygen atoms in the basal positions, and an apical vanadyl oxygen atom, defining a square base pyramid.

The nearest copper(II) centres are linked together by three bridges: two O–P–O bridges and one O–V–O bridge, involving vanadyl oxygen atoms, to form dimeric units with d_{Cu-Cu} = 4.481 Å. The copper(II) centres of the dimer are interconnected by a phosphovanadate ribbon by means of phosphate and vanadyl oxygen atoms. This ribbon is composed of a tetrametallic $V_4O_9^{2+}$ unit, formed by two μ_2-phosphate vanadium(V) dimers interconnected through a V–O–V bridge. Besides, each tetrameric unit is interconnected by phosphate groups, generating a chain-like structure in the ***a***-direction. In this way, a chain of dimers is formed (Fig. 2b). Phosphate groups are present on the periphery, either as HPO_4 or $H_2P_2O_7$, due to half occupancy on the phosphorus P3 site. These phosphate groups located on the periphery ensure additional links between adjacent chains, through hydrogen bonds generating a two-dimensional inorganic framework. The chelating bipy groups extend from the inorganic layer at an angle of *ca.* 76°. Additionally, each of these non-covalent layers interacts with its nearest neighbours through the stacking of the bipy fragments to produce a "zipper-like" crystal structure. The distance between the stacked bipy molecules is about 3.5 Å and is indicative of the presence of intermolecular interactions.

Compounds which contain both orthophosphate and diphosphate groups have been described previously mostly for vanadium(III) and (IV) compounds.[22] In the present work we have been able to isolate a vanadium(V) phosphate copper(II) complex (**2**), where both PO_4 tetrahedra and P_2O_7 groups coexist. Relevant geometrical parameters like bond distances, angles and dihedral angles are given in Table 2.

$[(Cu_2(dpa))_2(V_2P_2O_{12})]_n$ (4). Table 2 shows selected bond distances and angles for **4**. The structure of **4** is constructed of the dimeric $(Cu_2(dpa))_2(V_2P_2O_{12})$ unit (see Fig. 1c) forming an infinite covalent chain oriented along the ***a*** cell axis. The Cu(II) ion has a distorted square planar coordination sphere composed of two nitrogen atoms from the chelating dpa ligand and two oxygen atoms from two different phosphate groups. The $V_2P_2O_{12}^{4-}$ anion, which is formed by the corner sharing of VO_2^+ cations with PO_4^{3-} anions, acts as a bridge between two Cu(dpa) units using the phosphate oxygen atoms. The chain is then defined by the alternation of the phospho–vanadate anions and the Cu–dpa units (Fig. 2c). The distance between two nearest copper(II)–copper(II) neighbours inside the dimer is 5.035 Å and 7.396 Å along the chain. The distance of each copper(II) centre to the uncoordinated O6 of the VO_2^+ group is 2.905(2) Å. Every copper(II) centre deviates slightly (0.1 Å) from the least-squares plane defined by the chelating dpa ligand. The least-squares planes corresponding to two nearest neighbours copper centres are parallel (dihedral angle of 0°).

This chain pattern has been previously described by Finn and Zubieta for $[Cu(phen)(V_2P_2O_{12})]_n$,[23] with the difference that in this compound the vanadyl oxo atoms of $V_2P_2O_{12}$ are coordinated to the $Cu(diimine)^{2+}$ unit instead of the phosphate ones.

The individual chains are interpenetrated by the dpa ligands, that are perpendicular to the direction of the $\{(Cu(dpa))_2(V_2P_2O_{12})\}_n$ chain. The distance between the stacked dpa is about 3.7 Å. The interpenetration permits hydrogen bonding

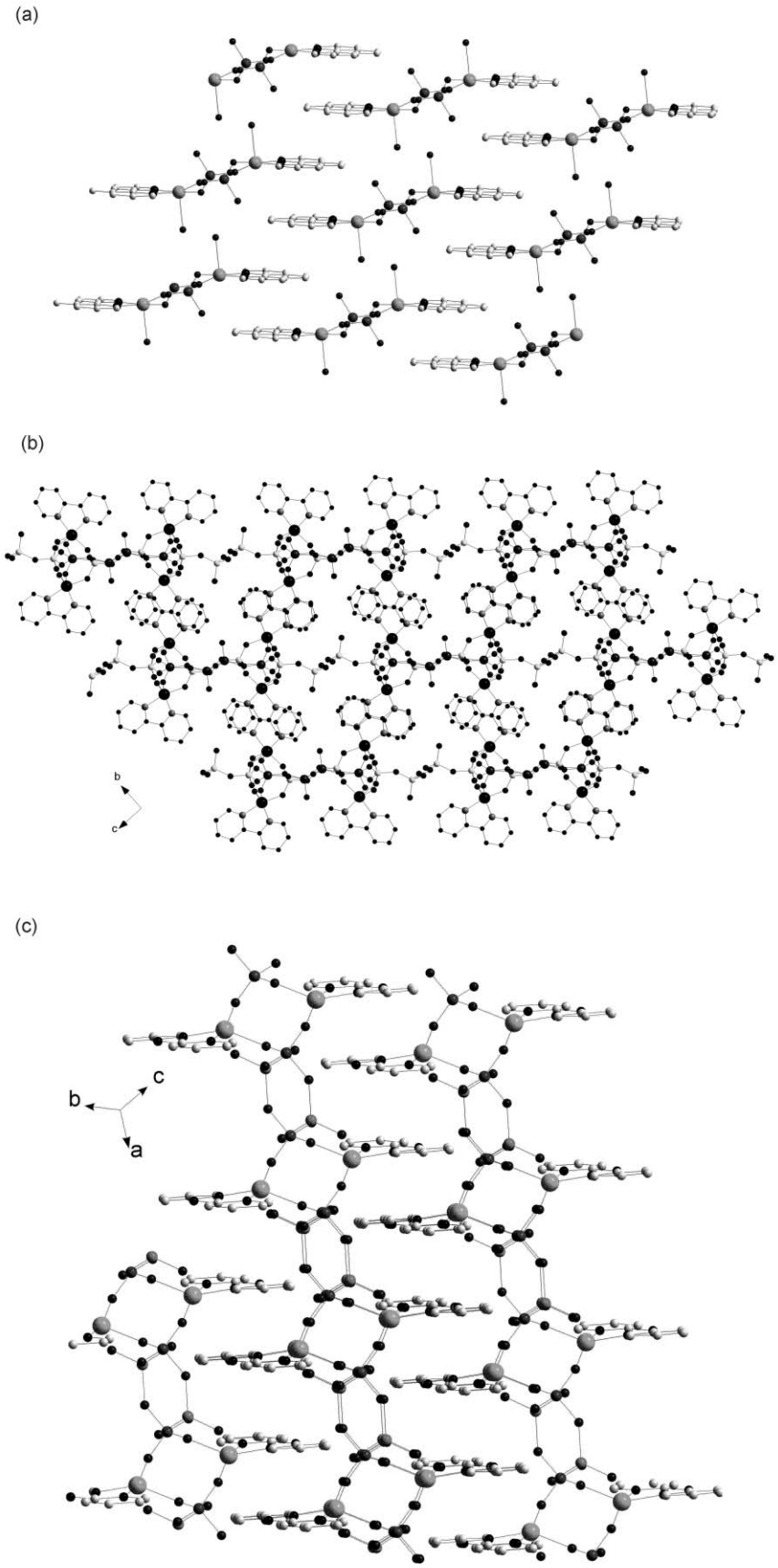

Fig. 2 Packing diagrams for a) $[Cu_2(phen)_2(H_2O)_2(H_2PO_4)_2](NO_3)_2{\cdot}2H_2O$ (**1**), b) $[(Cu_2(bipy)_2)_2(V_4O_9)(PO_4)_2(HPO_4)(H_2P_2O_7)]_n{\cdot}nH_2O$ (**2**) and c) $[(Cu(dpa))_2(V_2P_2O_{12})]_n$ (**4**).

interactions between the NH groups of the dpa ligands of one chain with the terminal oxo groups of the VO_4 tetrahedra of the vicinal chain, defining a "zipper-like" structure. The distances and angle involved are H1···O8, 1.85 Å; O4···O8, 2.82 Å; and O4···H1···O8: 164.1°. As a consequence a 2D hydrogen-bonded network is formed.

Although a variety of coordination geometries and connectivities are exhibited by the previously described series of

Table 2 Selected bond lengths (Å) and angles (°) for $[Cu_2(phen)_2(H_2O)_2(H_2PO_4)_2](NO_3)_2\cdot 2\ H_2O$ (**1**), $[(Cu_2(bipy)_2)_2(V_4O_9)(PO_4)_2(HPO_4)(H_2P_2O_7)]_n\cdot nH_2O$ (**2**) and $[(Cu(dpa))_2(V_2P_2O_{12})]_n$ (**4**).

$[Cu_2(phen)_2(H_2O)_2(H_2PO_4)_2](NO_3)_2\cdot 2H_2O$ (**1**)			
Cu–O4P	1.941(2)	Cu–O3P[a]	1.920(2)
Cu–N1	2.019(2)	Cu–N2	2.021(2)
Cu–O1W	2.308(2)		
O4P–Cu–N1	94.17(8)	O4P–Cu–N2	174.54(8)
N1–Cu–N2	81.51(8)	O4P–Cu–O1w	92.7(1)
N1–Cu–O1W	97.7(1)	N2–Cu–O1w	91.2(1)
$[(Cu_2(bipy)_2)_2(V_4O_9)(PO_4)_2(HPO_4)(H_2P_2O_7)]_n\cdot nH_2O$ (**2**)			
Cu1–O3	2.30(1)	Cu1–O7	1.971(8)
Cu1–O13	2.026(7)	Cu1–N1	2.014(8)
Cu1–N2	2.014(8)	Cu2–N3	2.01(1)
Cu2–N4	2.02(1)	Cu2–O12	1.949(8)
Cu2–O2	2.25(1)	Cu2–O9	1.957(8)
V1–O1	2.102(8)	V1–O2	1.584(8)
V1–O3	1.608(8)	V1–O4	1.972(7)
V1–O11	1.97(1)	V2–O8	1.934(9)
V2–O1	2.133(6)	V2–O4	1.923(8)
V2–O5	1.577(8)	V2–O6	1.760(2)
O7–Cu1–O3	98.0(3)	O7–Cu1–O13	92.5(3)
O7–Cu1–N2	95.3(3)	O7–Cu1–N1	163.7(4)
N2–Cu1–O3	84.7(4)	N1–Cu1–O3	97.8(4)
O9–Cu2–O2	87.1(3)	O9–Cu2–N4	165.7(4)
O9–Cu2–N3	91.8(4)	N4–Cu2–O2	103.6(4)
N3–Cu2–O2	90.7(4)	O3–V1–O1	93.1(4)
O2–V1–O1	91.4(4)	N3–Cu2–N4	78.7(4)
N2–Cu1–N1	81.8(4)	O3–V1–O11	122.6(4)
O2–V1–O3	109.0(4)	O3–V1–O13′	90.9(7)
O2–V1–O11	89.4(4)	O2–V1–O4	127.9(4)
O3–V1–O4	120.5(4)	O11–V1–O4	77.7(3)
O11–V1–O1	141.7(3)	O4–V2–O1	72.1(3)
O4–V1–O1	71.8(3)	O5–V2–O4	111.1(4)
O5–V2–O1	97.9(3)	O5–V2–O8	113.7(4)
O5–V2–O6	105.1(3)		
$[(Cu(dpa))_2(V_2P_2O_{12})]_n$ (**4**)			
Cu–O1	1.956(4)	Cu–O2[b]	1.896(4)
Cu–N1	1.964(5)	Cu–N3	1.979(5)
V–O3	1.830(4)	V–O5	1.590(5)
V–O6	1.589(5)	V–O4[c]	1.825(5)
N1–Cu–N3	92.3(2)	O1–Cu–N3	146.4(2)
O1–Cu–N1	94.7(2)	O2–Cu[b]–N1	156.3(2)
O2–Cu[b]–O1	94.8(2)	O2–Cu[b]–N3	91.7(2)
O5–V–O6	110.4(3)	O5–V–O3	110.7(2)
O6–V–O3	109.7(2)	O5–V–O4[c]	108.2(2)
O6–V–O4[c]	110.3(2)	P–O1–Cu	121.1(3)
P–O2–Cu[b]	148.6(3)		

[a] $-x+1, -y+1, -z$. [b] $-x, -y+1, -z+1$. [c] $-x-1, -y+1, -z+1$.

compounds, they are closely related in the sense that they are composed of dimeric copper(II) units. Additionally, in **2** and **4**, dimer chains are defined. The copper centres are bridged by phosphate, pyrophosphate and oxovanadium groups in **2**, while **1**, **3** and **4** present only O–P–O bridges. In compound **3** the vanadyl groups are only bonded to one copper centre.

It is important to emphasise that the structures of compounds **2** and **4** differ from the reported $[Cu_2(phen)_2(VO_2)_2(PO_4)_2]$[16] chain, even though all compounds have chelating diimine ligands which prevent the formation of 2D or 3D covalently linked structures. Several compounds are known in which these 3D structures are attained by the use of 4,4′-bipy or 4,4′-dpa ligands.[16,24]

b) Magnetic behaviour

As commented in the structural section, compounds **1–4** contain one unpaired electron Cu(II) ($3d^9$, $S = ½$) centre in a distorted-square (**4**) or square pyramidal environment (**1–3**),

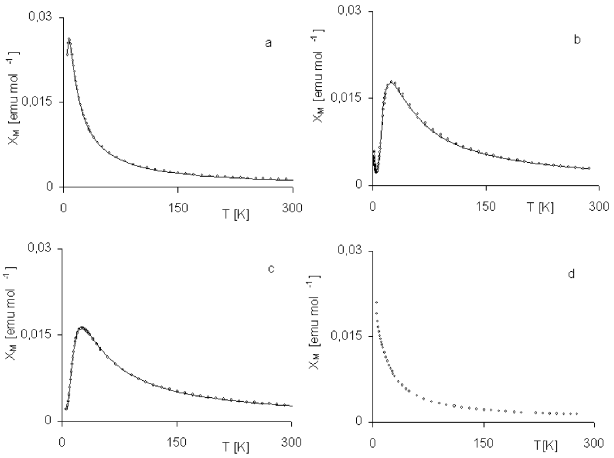

Fig. 3 Temperature dependence of the corrected molar susceptibility of compounds a) $[Cu_2(phen)_2(H_2O)_2(H_2PO_4)_2](NO_3)_2\cdot 2H_2O$ (**1**), b) $[(Cu_2(bipy)_2)_2(V_4O_9)(PO_4)_2(HPO_4)(H_2P_2O_7)]_n\cdot nH_2O$ (**2**), c) $[Cu_2(bipy)_2(VO_2)_2(PO_4)_2]_n$ (**3**) and d) $[(Cu(dpa))_2(V_2P_2O_{12})]_n$ (**4**).

bridged by phosphate and/or pyrophosphate and/or vanadyl bridges to define dimer (**1**) or dimer chains (**2–4**). Fig. 3 shows the temperature dependence of the molar magnetic susceptibility (χ_M) for the entire series of compounds **1–4**. The curves are characteristic of antiferromagnetic exchange coupling with susceptibility maxima at 8, 25 and 26 K for compounds **1**, **2** and **3** respectively. Taking into account the structural features of these copper compounds, the molar magnetic susceptibility curves were fitted using the Bleaney–Bowers expression, corrected for monomeric impurities with Curie behaviour[25] according to $\chi_M = (1-\rho)\chi_{dim.} + \rho\chi_{mono.}$ with $\chi_{dim} = 2Ng^2\beta^2[kT(3+\exp(-J/kT)]^{-1}$ and $\chi_{mono.} = Ng^2\beta^2S(S+1)/(3kT)$, where N, g, β, k have their usual meaning; J is the exchange coupling constant and ρ is the monomeric impurity fraction. The best fits were obtained for $J = -8.0$ cm^{-1}, $g = 2.0$ and $\rho = 0.01$ for **1**; $J = -28.8$ cm^{-1}, $g = 2.25$, $\rho = 0.025$ for **2**; $J = -29.0$ cm^{-1}, $g = 2.12$ and $\rho = 0.023$ for **3**.

Additionally, for compounds **2** and **3**, the alternating chain model was used to fit the magnetic susceptibility data with $\chi = 2Ng^2\beta^2(A+Bx+Cx^2)[kT(1+Dx+Ex^2+Fx^3)]^{-1}$ where coefficients A–F are functions of the alternation parameter α along the chain and $x = J/kT$.[25] This model fits the experimental data when a weak ferromagnetic coupling is considered between the dimeric units ($\alpha = -0.03$ for **2** and -0.027 for **3**). The resulting intradimer J values (-28.8 cm^{-1} for **2** and -29.4 cm^{-1} for **3**) compare well with the Bleaney–Bowers model values. The interdimer J' values calculated with the above data are of the order of $+1$ cm^{-1} (0.87 cm^{-1} for **2**, 0.79 cm^{-1} for **3**).

Compound **4** presents, between 20 and 300 K, magnetic behaviour, which can be well characterised by means of the Curie–Weiss law with $\mu = 1.79$ BM and $\theta = -23$ K. Surprisingly we did not observe a maximum in the susceptibility data down to 5 K even though θ is almost -23 K. Efforts to fit the magnetic data to the dimer or alternating chain models were unsuccessful.

Since the compounds described in this work present a variety of connectivities between the unpaired electron centres, it is necessary to analyse the factors governing the magnetic exchange through the phosphato–vanadyl bridges.

Scheme 1 shows a schematic picture of the geometrical parameters that may have some influence on the magnetic coupling inside the bridged dimers. Three kinds of planes can be defined in the system: one corresponding to the copper coordination plane, another to the O–P–O bridge, and finally one corresponding to the four coordinated phosphate oxygen atoms, respectively named ***A***, ***B*** and ***C***. Table 3 presents a

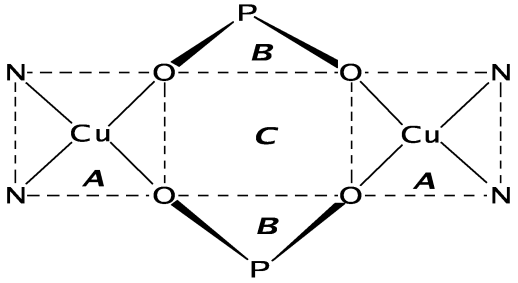

Scheme 1 Structural details of the planes ***A***, ***B*** and ***C***.

summary of relevant structural data for the magnetic discussion.

First let us consider the magnetically diluted compound **4**. In our opinion the absence of significant intradimer coupling in **4** can be ascribed to the strong tetrahedral distortion of the square planar geometry. This fact permits the mixing of the d_{x2-y2} orbital with other d-set orbitals, precluding magnetic coupling through the bridges.

With respect to the magnetically coupled compounds, the simplest analysis corresponds to dimeric units. Recently Julve *et al.* reported on the antiferromagnetic coupling in the pyrophosphate-bridged copper(II) complex $[Cu_2(bipy)_2(H_2O)_2(P_2O_7)]\cdot 7H_2O$[26] which shows the same connectivity as **1** (Table 3). In both compounds the coordination geometry corresponds to a square base pyramid with O–P–O connecting the copper(II) centres at the basal position. The main difference between the pyrophosphate bridged compound and **1** lies in the fact that, in the former, the two O–P–O bridges are part of one P_2O_7 unit, determining a boat like conformation for the Cu–O–P–O–Cu–O–P–O unit, while a chair-like conformation is found in **1**.

There is no obvious relationship between the value of the bridging angles and the observed magnitude of the antiferromagnetic coupling exchange (Table 3). From the data presented in this table, it becomes obvious that different torsions of the copper–ligand planes make comparison difficult. Thus, the concept of maximum overlap of magnetic orbitals necessary for the presence of a strong antiferromagnetic exchange interaction developed by Kahn,[25] and later corroborated by Alvarez *et al.*[27] through calculations on -OR bridged copper(II) dimers with planar geometry, is not useful in our analysis.

While the above mentioned binuclear 0D compounds present only O–P–O bridges, compounds **2** and **3** present both PO_4 tetrahedra and vanadium polyhedra participating in the bond formation with the Cu(bipy) fragments. These two 1D compounds show a slightly larger antiferromagnetism, which suggests that the oxovanadium(V) fragment plays an electronic role that modifies to some extent the electronic structure of the phosphate group favouring the antiferromagnetic coupling through this anion. Oxovanadium groups have been reported to act as a pathway for magnetic coupling.[28]

Conclusions

New 0D and 1D compounds were synthesised by the hydrothermal method. Even though a reducing medium was used (Zn), all the isolated species were copper(II) and vanadium(V) compounds. We herein report a new example of a vanadium(V) species in which both PO_4 and P_2O_7 groups coexist.[29]

All the studied compounds with copper(II) atoms in a square pyramidal geometry present intradimer antiferromagnetism, while compound **4** in which the copper(II) atoms are in a highly distorted square planar geometry behaves as a paramagnet.

The series of compounds described in this paper clearly

Table 3 Summary of the structural and magnetic data

Compound	Cu(II) Geom.[a]	Dihedral angles/°			Bond angles/°		d_{Cu-Cu}/Å	μ/BM	θ/K	T_{max}/K	J/cm^{-1}	g	ρ
		A–B	*A–C*	*B–C*	Cu–O–P	O–P–O							
$[Cu_2(phen)_2(H_2PO_4)_2](NO_3)_2\cdot 2H_2O$ (**1**)	S-P CC	52.3	150.8	121.2	135.1	115.1	5.01	1.82	−7.2	8	−8.0	2.00	0.01
$[Cu_2(bipy)_2(H_2O)_2(P_2O_7)]$[26]	S-P BC	84.3 84.4 86.0 87.2	48.6 3.3	89.1 90.4	126.17 128.24 128.73 125.8	93.31/94.97	4.647	—	—	19	−20.0	2.09	—
$[(Cu_2(bipy)_2)_2(V_4O_9)(PO_4)_2(H_2P_2O_7)_2]_n\cdot nH_2O$ (**2**)	S-P CC	74.1	43.4	53.6	132.0	113.2 109.4	4.481	1.97	−19.8	25	−28.8	2.25	0.025
$[Cu_2(bipy)_2(VO_2)_2(PO_4)_2]_n$ (**3**)	S-P CC	63.3	14.8	70.0	139.3/124.8	114.2	5.06	1.88	−19.0	26	−29.0	2.12	0.023
$[(Cu(dpa))_2(V_2P_2O_{12})]_n$ (**4**)	D-SP CC	89.6	21.0	68.7	120.0/148.0	114.7	5.03	1.79	−23.0	—	—	—	—

[a]S-P: square pyramidal; D-SP: distorted square planar; CC: chair conformation; BC: boat conformation; J, g and ρ: dimer model.

illustrates how far geometry can modify magnetic coupling between Cu(II) centres bridged by O–P–O groups. They also suggest that the ability of these fragments to transmit magnetic exchange can be modified by oxovanadium centres connected to them.

Acknowledgements

The authors acknowledge financial support from FONDAP (grant 11980002), CNRS/CONICYT (programs 10071 and 11952) and PICS 922. We are also grateful to Fundacion Andes for supporting the purchase of the SMART APEX system currently operating at the University of Chile.

References

1 M. E. Leonowicz, J. W. Johnson, J. F. Brody, H. F. Shannon and J. M. Newsam, *J. Solid. State Chem.*, 1985, **56**, 370.
2 E. Le Fur, Y. Moreno and J.-Y. Pivan, *J. Mater. Chem.*, 2001, **11**, 1735.
3 F. Berrah, A. Guesdon, A. Leclaire, M.-M. Borel, J. Provost and B. Raveau, *Solid State Sci.*, 2001, **3**, 477.
4 E. Le Fur, A. Riou, O. Peña and J.-Y. Pivan, *Solid State Sci.*, 2000, **2**, 135.
5 Z. Bircsak and W. T. A. Harrison, *Inorg. Chem.*, 1998, **37**, 3204.
6 M. I. Khan, Q. Chen and J. Zubieta, *Inorg. Chim. Acta*, 1993, **213**, 328.
7 Y. Xu, L. H. An and L. L. Koh, *Chem. Mater.*, 1996, **8**, 814.
8 M. E. Davis and R. F. Lobo, *Chem. Mater.*, 1992, **4**, 756.
9 Y. Zhang, C. J. O'Connor, A. Clearfield and R. C. Haushalter, *Chem. Mater.*, 1996, **8**, 595.
10 H. Guohne, J. W. Johnson, A. J. Jacobson and J. S. Merola, *J. Solid. State Chem.*, 1991, **91**, 385.
11 P. J. Zapf, R. C. Haushalter and J. Zubieta, *Chem. Mater.*, 1997, **9**, 2019.
12 Y. Zhang, P. J. Zapf, L. M. Meyer, R. C. Haushalter and J. Zubieta, *Inorg. Chem.*, 1997, **36**, 2159.
13 P. J. Zapf, C. J. Warren, R. C. Haushalter and J. Zubieta, *Chem. Commun.*, 1997, 1543.
14 P. J. Hagrman, D. Hagrman and J. Zubieta, *Angew. Chem., Int. Ed.*, 1999, **38**, 2639.
15 Z. Shi, S. Feng, S. Gao, L. Zhang, G. Yang and J. Hua, *Angew. Chem., Int. Ed.*, 2000, **39**, 2325.
16 Z. Shi, S. Feng, L. Zhang, G. Yang and J. Hua, *Chem. Mater.*, 2000, **12**, 2930.
17 Y. Zhan, R. C. Haushalter and J. Zubieta, *Inorg. Chim. Acta*, 1997, **260**, 105.
18 SAINTPLUS V.6.02 Brüker AXS, Madison, WI, 1999.
19 SHELXTL V 5.1 Brüker AXS, Madison, WI 1998; G. M. Sheldrick, *SHELXL-97, Program for refinement of crystal structures*, University of Göttingen, Germany, 1997.
20 A. Altomare, M. C. Burla, M. Camalli, G. L. Cascarano, C. Giacovazzo, A. Guagliardi, A. G. G. Moliterni, G. Polidori and R. Spagna, *J. Appl. Crystallogr.*, 1999, **32**, 115.
21 V. Petricek and M. Dusek, Jana2000: Crystallographic computing system for ordinary and modulated structures, *J. Appl. Crystallogr.*, 2001, **34**, 398; available free at http://www-xray.fzu.cz/jana/jana.html.
22 S. Boudin, A. Guesdon, A. Leclaire and M.-M. Borel, *Int. J. Inorg. Mater.*, 2000, **2**, 561.
23 R. C. Finn and J. Zubieta, *J. Phys. Chem. Solids*, 2001, **62**, 1513.
24 L. I. Hung, S. L. Wang, H. M. Kao and K. H. Lii, *Inorg. Chem.*, 2002, **41**, 3929.
25 O. Kahn, *Molecular Magnetism*, Wiley-VCH, New York, 1993.
26 P. E. Kruger, R. P. Doyle, M. Julve, F. Lloret and M. Nieuwenhuyzen, *Inorg. Chem.*, 2001, **40**, 1726.
27 E. Ruiz, P. Alemany, S. Alvarez and J. Cano, *J. Am. Chem. Soc.*, 1997, **119**, 1297.
28 J. R. D. De Bord, Y. Zhang, R. C. Haushalter, J. Zubieta and C. J. O'Connor, *J. Solid State Chem.*, 1996, **122**, 251.
29 E. Le Fur, B. de Villars, J. Tortelier and J.-Y. Pivan, *Int. J. Inorg. Mater.*, 2001, **3**, 341.